PERISTALTIC MOTION OF A JOHNSON-SEGALMAN FLUID IN A PLANAR CHANNEL

T. HAYAT, Y. WANG, A. M. SIDDIQUI, AND K. HUTTER

Received 22 July 2002

This paper is devoted to the study of the two-dimensional flow of a Johnson-Segalman fluid in a planar channel having walls that are transversely displaced by an infinite, harmonic travelling wave of large wavelength. Both analytical and numerical solutions are presented. The analysis for the analytical solution is carried out for small Weissenberg numbers. (A Weissenberg number is the ratio of the relaxation time of the fluid to a characteristic time associated with the flow.) Analytical solutions have been obtained for the stream function from which the relations of the velocity and the longitudinal pressure gradient have been derived. The expression of the pressure rise over a wavelength has also been determined. Numerical computations are performed and compared to the perturbation analysis. Several limiting situations with their implications can be examined from the presented analysis.

1. Introduction

The dynamics of the fluid transport by peristaltic motion of the confining walls has received a careful study in the recent literature. The need for peristaltic pumping may arise in circumstances where it is desirable to avoid using any internal moving parts such as pistons in a pumping process. Moreover, the peristalsis is also well known to the physiologists to be one of the main mechanisms of fluid transport in a biological system. Specifically, peristaltic mechanism is involved in swallowing food through the oesophagus, urine transport from the kidney to the bladder through the ureter, movement of chyme in the gastrointestinal tract, and transport of spermatozoa in the ductus efferentes of the male reproductive tracts. Moreover, in the cervical canal, it is involved in the movement of ovum in the Fallopian tube, transport of lump in the lymphatic vessels, and vasomotion of small blood vessels such as arterioles, venules, and capillaries, as well as in the mechanical and neurological aspects of the peristaltic reflex. In plant physiology, such a mechanism is involved in phloem translocation by driving a sucrose solution along tubules by peristaltic contractions. In addition, peristaltic pumping occurs in many practical applications involving biomechanical systems such as roller and finger pumps. The

Mathematical Problems in Engineering 2003:1 (2003) 1–23
2000 Mathematics Subject Classification: 76A05, 76Z05
URL: http://dx.doi.org/10.1155/S1024123X03308014

application of peristaltic motion as a mean of transporting fluid has also aroused interest in engineering fields [1, 8, 30]. In particular, the peristaltic pumping of corrosive fluids and slurries could be useful as it is desirable to prevent their contact with mechanical parts of the pump.

Various studies (experimental as well as theoretical) on peristaltic transport have been carried out by many researchers in order to explore a variety of relevant information. In most of these studies, the peristaltic motion of a single fluid was considered by assuming the nature of the fluid to be Newtonian. Some of the previous researchers (cf. Burns and Parkes [4] and Shapiro et al. [25]) use the long wavelength approximation to simplify the mathematical complexities involved in the analysis, whereas some others (cf. Fung and Yih [6] and Chow [5]) applied perturbation techniques in their analyses. Misra and Pandey [18] also used the perturbation technique to put forward a mathematical analysis for flows through nonuniform tubes in the context of physiological fluid dynamics and found that their results are in a good agreement with experimental data of Guha et al. [7]. A summary of analytical papers up to 1984 has been presented by L. M. Srivastava and V. P. Srivastava [29]. Numerical techniques were used by Brown and Hung [3], Takabatake and Ayukawa [30] for channel flow, and Takabatake et al. [31] for axisymmetric tube flow.

Since physiological fluids are mostly of non-Newtonian nature, it is appropriate to study the dynamics of the fluids by taking their non-Newtonian behavior into consideration. Only limited information on the peristaltic transport of non-Newtonian fluids is available (L. M. Srivastava and V. P. Srivastava [29], Böhme and Friedrich [2], Raju and Devanathan [20, 21], Misra and Pandey [19], Siddiqui et al. [26], and Siddiqui and Schwarz [27, 28]).

In this paper, we study the peristaltic motion of Johnson-Segalman fluids. The Johnson-Segalman model is a viscoelastic fluid model which was developed to allow for non-affine deformations [9]. Recently, this model has been used by a number of researchers [10, 13, 15] to explain the "spurt" phenomenon. Experimentalists usually associate a spurt with a slip at the wall, and on this issue experiments have been carried out [11, 12, 14, 16, 17, 22]. Recently, Rao and Rajagopal [24] discussed three distinct flows of a Johnson-Segalman fluid. The three flows are cylindrical Poiseuille flows. In another paper, Rao [23] examined the flow of a Johnson-Segalman fluid between rotating coaxial cylinders with and without suction. Unlike most other fluid models, the Johnson-Segalman fluid allows for a nonmonotonic relationship between the shear stress and the rate of share in a simple shear flow for certain values of the material parameter. Keeping this in view, the nonlinear partial differential equations for the peristalsis of a Johnson-Segalman fluid are modelled. Due to the complexity of the nonlinear equations, we only consider the case of planar flow, which is a symmetric, harmonic, infinite wave train having long wavelength. We give the basic equations in Section 2. The formulation of the problem is given in Section 3. In Section 4, we derive the boundary conditions. Section 5 is devoted to the partial differential equations with long-wavelength approximation. As the problem is complicated, it is solved by the perturbation technique in Section 6. The perturbation solution is made of two parts: a mean part corresponding to the fully developed mean flow and small disturbance. It is worth mentioning here that the mean part

of the solution describes the flow characteristics in the case of a Newtonian fluid. The perturbed parts of the solution are the contributions from the Johnson-Segalman fluid. Section 7 is concerned with the numerical solution of the nonlinear partial differential equation. In Section 8, numerical results and discussions are given. The analytical results are also compared to a numerical computation in order to determine the range of validity of the perturbation analysis.

2. Basic equations

The basic equations governing the flow of an incompressible fluid are the field equations

$$\operatorname{div}\mathbf{V} = 0, \qquad \operatorname{div}\boldsymbol{\sigma} + \rho\mathbf{f} = \rho\frac{d\mathbf{V}}{dt}, \tag{2.1}$$

where $\mathbf{V}$ is the velocity, $\mathbf{f}$ the body force per unit mass, ρ the density, d/dt the material time derivative, and $\boldsymbol{\sigma}$ is the Cauchy stress.

Johnson and Segalman [9] proposed an integral model which can also be written in the rate-type form. With an appropriate choice of kernel function and the time constants, the Cauchy stress $\boldsymbol{\sigma}$ in such a Johnson-Segalman fluid is related to the fluid motion through

$$\boldsymbol{\sigma} = -p\mathbf{I} + \mathbf{T}, \tag{2.2}$$

$$\mathbf{T} = 2\mu\mathbf{D} + \mathbf{S}, \tag{2.3}$$

$$\mathbf{S} + m\left[\frac{d\mathbf{S}}{dt} + \mathbf{S}(\mathbf{W} - a\mathbf{D}) + (\mathbf{W} - a\mathbf{D})^{T}\mathbf{S}\right] = 2\eta\mathbf{D}, \tag{2.4}$$

where $\mathbf{D}$ is the symmetric part of the velocity gradient and $\mathbf{W}$ the skew-symmetric part of the velocity gradient, that is,

$$\mathbf{D} = \frac{1}{2}[\mathbf{L} + \mathbf{L}^{T}], \quad \mathbf{W} = \frac{1}{2}[\mathbf{L} - \mathbf{L}^{T}], \quad \mathbf{L} = \operatorname{grad}\mathbf{V}. \tag{2.5}$$

Also, $-p\mathbf{I}$ denotes the indeterminate part of the stress due to the constraint of incompressibility, μ and η are viscosities, m is the relaxation time, and a is called the slip parameter. When $a = 1$, the Johnson-Segalman model reduces to the Oldroyd-B model; when $a = 1$ and $\mu = 0$, the Johnson-Segalman model reduces to the Maxwell fluid; and when $m = 0$, the model reduces to the classical Navier-Stokes fluid. Note that the bracketed term on the left-hand side of (2.4) is an objective time derivative.

3. Formulation of the problem and flow equations

Consider a two-dimensional infinite channel of uniform width $2n$ filled with an incompressible Johnson-Segalman fluid. We choose a rectangular coordinate system for the channel with $\bar{X}$ along the center line and $\bar{Y}$ normal to it. Let $\bar{U}$ and $\bar{V}$ be the longitudinal and transverse velocity components of the fluid, respectively. We assume that an infinite train of sinusoidal waves progresses with velocity c along the walls in the $\bar{X}$-direction. The

geometry of the wall surface is defined as

$$\bar{h}(\bar{X},t) = n + b\sin\left(\frac{2\pi}{\lambda}(\bar{X}-ct)\right), \tag{3.1}$$

where b is the amplitude and λ is the wavelength. We also assume that there is no motion of the wall in the longitudinal direction (extensible or elastic wall).

For unsteady two-dimensional flows,

$$\mathbf{V} = \left[\bar{U}(\bar{X},\bar{Y},t), \bar{V}(\bar{X},\bar{Y},t), 0\right], \tag{3.2}$$

the equations of motion (2.1) and the constitutive relations (2.2), (2.3), and (2.4) in the absence of body forces take the following form:

$$\frac{\partial \bar{U}}{\partial \bar{X}} + \frac{\partial \bar{V}}{\partial \bar{Y}} = 0, \tag{3.3}$$

$$\rho\left(\frac{\partial}{\partial t} + \bar{U}\frac{\partial}{\partial \bar{X}} + \bar{V}\frac{\partial}{\partial \bar{Y}}\right)\bar{U} = -\frac{\partial \bar{p}(\bar{X},\bar{Y},t)}{\partial \bar{X}} + \mu\left(\frac{\partial^2}{\partial \bar{X}^2} + \frac{\partial^2}{\partial \bar{Y}^2}\right)\bar{U} + \frac{\partial \bar{S}_{\bar{X}\bar{X}}}{\partial \bar{X}} + \frac{\partial \bar{S}_{\bar{X}\bar{Y}}}{\partial \bar{Y}}, \tag{3.4}$$

$$\rho\left(\frac{\partial}{\partial t} + \bar{U}\frac{\partial}{\partial \bar{X}} + \bar{V}\frac{\partial}{\partial \bar{Y}}\right)\bar{V} = -\frac{\partial \bar{p}(\bar{X},\bar{Y},t)}{\partial \bar{Y}} + \mu\left(\frac{\partial^2}{\partial \bar{X}^2} + \frac{\partial^2}{\partial \bar{Y}^2}\right)\bar{V} + \frac{\partial \bar{S}_{\bar{X}\bar{Y}}}{\partial \bar{X}} + \frac{\partial \bar{S}_{\bar{Y}\bar{Y}}}{\partial \bar{Y}}, \tag{3.5}$$

$$2\eta\frac{\partial \bar{U}}{\partial \bar{X}} = \bar{S}_{\bar{X}\bar{X}} + m\left[\frac{\partial}{\partial t} + \bar{U}\frac{\partial}{\partial \bar{X}} + \bar{V}\frac{\partial}{\partial \bar{Y}}\right]\bar{S}_{\bar{X}\bar{X}} - 2am\bar{S}_{\bar{X}\bar{X}}\frac{\partial \bar{U}}{\partial \bar{X}} + m\left[(1-a)\frac{\partial \bar{V}}{\partial \bar{X}} - (1+a)\frac{\partial \bar{U}}{\partial \bar{Y}}\right]\bar{S}_{\bar{X}\bar{Y}}, \tag{3.6}$$

$$\eta\left(\frac{\partial \bar{U}}{\partial \bar{Y}} + \frac{\partial \bar{V}}{\partial \bar{X}}\right) = \bar{S}_{\bar{X}\bar{Y}} + m\left[\frac{\partial}{\partial t} + \bar{U}\frac{\partial}{\partial \bar{X}} + \bar{V}\frac{\partial}{\partial \bar{Y}}\right]\bar{S}_{\bar{X}\bar{Y}} + \frac{m}{2}\left[(1-a)\frac{\partial \bar{U}}{\partial \bar{Y}} - (1+a)\frac{\partial \bar{V}}{\partial \bar{X}}\right]\bar{S}_{\bar{X}\bar{X}} + \frac{m}{2}\left[(1-a)\frac{\partial \bar{V}}{\partial \bar{X}} - (1+a)\frac{\partial \bar{U}}{\partial \bar{Y}}\right]\bar{S}_{\bar{Y}\bar{Y}}, \tag{3.7}$$

$$2\eta\frac{\partial \bar{V}}{\partial \bar{Y}} = \bar{S}_{\bar{Y}\bar{Y}} + m\left[\frac{\partial}{\partial t} + \bar{U}\frac{\partial}{\partial \bar{X}} + \bar{V}\frac{\partial}{\partial \bar{Y}}\right]\bar{S}_{\bar{Y}\bar{Y}} - 2am\bar{S}_{\bar{Y}\bar{Y}}\frac{\partial \bar{V}}{\partial \bar{Y}} + m\left[(1-a)\frac{\partial \bar{U}}{\partial \bar{Y}} - (1+a)\frac{\partial \bar{V}}{\partial \bar{X}}\right]\bar{S}_{\bar{X}\bar{Y}}. \tag{3.8}$$

In the fixed coordinate system $(\bar{X},\bar{Y})$, the motion is unsteady because of the moving boundary. However, if observed in a coordinate system $(\bar{x},\bar{y})$ moving with the speed c, it can be treated as steady because the boundary shape appears to be stationary. The transformation between the two frames is given by

$$\bar{x} = \bar{X} - ct, \qquad \bar{y} = \bar{Y}. \tag{3.9}$$

The velocities in the fixed and moving frames are related by

$$\bar{u} = \bar{U} - c, \qquad \bar{v} = \bar{V}, \tag{3.10}$$

where $(\bar{u},\bar{v})$ are components of the velocity in the moving coordinate system.

We use these transformations and define the following dimensionless variables:

$$x=\frac{2\pi}{\lambda}\bar{x},\qquad y=\frac{\bar{y}}{n},\qquad u=\frac{\bar{u}}{c},\qquad v=\frac{\bar{v}}{c},$$
$$S=\frac{n}{\mu c}\bar{S},\qquad p=\frac{2\pi n^2}{\lambda(\mu+\eta)c}\bar{p},\qquad h=\frac{\bar{h}}{n},\tag{3.11}$$

where the wavelength λ is the characteristic longitudinal length. Substituting (3.9) and (3.10) into (3.3), (3.4), (3.5), (3.6), (3.7), and (3.8), and then using dimensionless variables (3.11), we arrive at

$$\delta\frac{\partial u}{\partial x}+\frac{\partial v}{\partial y}=0,\tag{3.12}$$

$$\Re\mathrm{e}\left[\left(\delta u\frac{\partial}{\partial x}+v\frac{\partial}{\partial y}\right)u\right]=\left(\frac{\mu+\eta}{\mu}\right)\frac{\partial p}{\partial x}+\delta\frac{\partial S_{xx}}{\partial x}+\frac{\partial S_{xy}}{\partial y}+\left(\delta^2\frac{\partial^2 u}{\partial x^2}+\frac{\partial^2 u}{\partial y^2}\right),\tag{3.13}$$

$$\delta\Re\mathrm{e}\left[\left(\delta u\frac{\partial}{\partial x}+v\frac{\partial}{\partial y}\right)v\right]=-\left(\frac{\mu+\eta}{\mu}\right)\frac{\partial p}{\partial y}+\delta^2\frac{\partial S_{xy}}{\partial x}+\delta\frac{\partial S_{yy}}{\partial y}+\delta\left(\delta^2\frac{\partial^2 v}{\partial x^2}+\frac{\partial^2 v}{\partial y^2}\right),\tag{3.14}$$

$$\delta\left(\frac{2\eta}{\mu}\right)\frac{\partial u}{\partial x}=S_{xx}+\mathcal{W}\mathrm{e}\left[\delta u\frac{\partial}{\partial x}+v\frac{\partial}{\partial y}\right]S_{xx}-2\mathcal{W}\mathrm{e}\,a\delta\frac{\partial u}{\partial x}+\mathcal{W}\mathrm{e}\left[\delta(1-a)\frac{\partial v}{\partial x}-(1+a)\frac{\partial u}{\partial y}\right]S_{xy},\tag{3.15}$$

$$\frac{\eta}{\mu}\left(\frac{\partial u}{\partial y}+\delta\frac{\partial v}{\partial x}\right)=S_{xy}+\mathcal{W}\mathrm{e}\left[\delta u\frac{\partial}{\partial x}+v\frac{\partial}{\partial y}\right]S_{xy}+\frac{\mathcal{W}\mathrm{e}}{2}\left[(1-a)\frac{\partial u}{\partial y}-\delta(1+a)\frac{\partial v}{\partial x}\right]S_{xx}+\frac{\mathcal{W}\mathrm{e}}{2}\left[\delta(1-a)\frac{\partial v}{\partial x}-(1+a)\frac{\partial u}{\partial y}\right]S_{yy},\tag{3.16}$$

$$\left(\frac{2\eta}{\mu}\right)\frac{\partial v}{\partial y}=S_{yy}+\mathcal{W}\mathrm{e}\left[\delta u\frac{\partial}{\partial x}+v\frac{\partial}{\partial y}\right]S_{yy}-2\mathcal{W}\mathrm{e}\,aS_{yy}\frac{\partial v}{\partial y}+\mathcal{W}\mathrm{e}\left[(1-a)\frac{\partial u}{\partial y}-(1+a)\delta\frac{\partial v}{\partial x}\right]S_{xy},\tag{3.17}$$

in which the dimensionless wave number δ, the Reynolds number $\Re\mathrm{e}$, and the Weissenberg number $\mathcal{W}\mathrm{e}$ are defined, respectively, as

$$\delta=\frac{2\pi n}{\lambda},\quad \Re\mathrm{e}=\frac{\rho cn}{\mu},\quad \mathcal{W}\mathrm{e}=\frac{mc}{n}.\tag{3.18}$$

Equation (3.12) allows the introduction of the dimensionless stream function $\Psi(x,y)$ in terms of

$$u=\frac{\partial\Psi}{\partial y},\qquad v=-\delta\frac{\partial\Psi}{\partial x}.\tag{3.19}$$

In terms of Ψ, we find that (3.12) is identically satisfied, while the other equations take the forms

$$\delta \mathcal{R}\mathrm{e}\left[\left(\frac{\partial\Psi}{\partial y}\frac{\partial}{\partial x}-\frac{\partial\Psi}{\partial x}\frac{\partial}{\partial y}\right)\frac{\partial\Psi}{\partial y}\right]=-\left(\frac{\mu+\eta}{\mu}\right)\frac{\partial p}{\partial x}+\delta\frac{\partial S_{xx}}{\partial x}+\frac{\partial S_{xy}}{\partial y}+\left(\delta^2\frac{\partial^3\Psi}{\partial x^2\partial y}+\frac{\partial^3\Psi}{\partial y^3}\right),$$

$$-\delta^3 \mathcal{R}\mathrm{e}\left[\left(\frac{\partial\Psi}{\partial y}\frac{\partial}{\partial x}-\frac{\partial\Psi}{\partial x}\frac{\partial}{\partial y}\right)\frac{\partial\Psi}{\partial x}\right]=-\left(\frac{\mu+\eta}{\mu}\right)\frac{\partial p}{\partial y}+\delta^2\frac{\partial S_{xy}}{\partial x}+\delta\frac{\partial S_{yy}}{\partial y}-\delta^2\left(\delta^2\frac{\partial^3\Psi}{\partial x^3}+\frac{\partial^3\Psi}{\partial x\partial y^2}\right),$$

$$\left(\frac{2\eta\delta}{\mu}\right)\frac{\partial^2\Psi}{\partial x\partial y}=S_{xx}+\mathcal{W}\mathrm{e}\,\delta\left[\frac{\partial\Psi}{\partial y}\frac{\partial}{\partial x}-\frac{\partial\Psi}{\partial x}\frac{\partial}{\partial y}\right]S_{xx}-2\mathcal{W}\mathrm{e}\,a\delta\frac{\partial^2\Psi}{\partial x\partial y}$$
$$-\mathcal{W}\mathrm{e}\left[\delta^2(1-a)\frac{\partial^2\Psi}{\partial x^2}+(1+a)\frac{\partial^2\Psi}{\partial y^2}\right]S_{xy},$$

$$\frac{\eta}{\mu}\left(\frac{\partial^2\Psi}{\partial y^2}-\delta^2\frac{\partial^2\Psi}{\partial x^2}\right)=S_{xy}+\mathcal{W}\mathrm{e}\,\delta\left[\frac{\partial\Psi}{\partial y}\frac{\partial}{\partial x}-\frac{\partial\Psi}{\partial x}\frac{\partial}{\partial y}\right]S_{xy}+\frac{\mathcal{W}\mathrm{e}}{2}\left[(1-a)\frac{\partial^2\Psi}{\partial y^2}+\delta^2(1+a)\frac{\partial^2\Psi}{\partial x^2}\right]S_{xx}$$
$$-\frac{\mathcal{W}\mathrm{e}}{2}\left[\delta^2(1-a)\frac{\partial^2\Psi}{\partial x^2}+(1+a)\frac{\partial^2\Psi}{\partial y^2}\right]S_{yy},$$

$$-\left(\frac{2\eta\delta}{\mu}\right)\frac{\partial^2\Psi}{\partial x\partial y}=S_{yy}+\mathcal{W}\mathrm{e}\,\delta\left[\frac{\partial\Psi}{\partial y}\frac{\partial}{\partial x}-\frac{\partial\Psi}{\partial x}\frac{\partial}{\partial y}\right]S_{yy}+2\mathcal{W}\mathrm{e}\,a\delta S_{yy}\frac{\partial^2\Psi}{\partial x\partial y}$$
$$+\mathcal{W}\mathrm{e}\left[(1-a)\frac{\partial^2\Psi}{\partial y^2}+(1+a)\delta^2\frac{\partial^2\Psi}{\partial x^2}\right]S_{xy}. \tag{3.20}$$

4. Rate of volume flow and boundary conditions

The dimensional rate of fluid flow in the fixed frame is given by

$$Q=\int_0^{\bar{h}}\bar{U}(\bar{X},\bar{Y},t)d\bar{Y}, \tag{4.1}$$

where $\bar{h}$ is a function of $\bar{X}$ and t. The rate of fluid flow in the moving frame is given by

$$q=\int_0^{\bar{h}}\bar{u}(\bar{x},\bar{y})d\bar{y}, \tag{4.2}$$

where $\bar{h}$ is a function of $\bar{x}$ alone. With the help of (3.9) and (3.10), one can show that these two rates are related through

$$Q=q+c\bar{h}. \tag{4.3}$$

The time-averaged flow over a period T at a fixed position $\bar{X}$ is given by

$$\bar{Q}=\frac{1}{T}\int_0^T Q\,dt. \tag{4.4}$$

Substituting (4.3) into (4.4), we find that

$$\bar{Q}=Q+cn. \tag{4.5}$$

If we define the dimensionless time averaged flows Θ and F, respectively, in the fixed and moving frame as

$$\Theta = \frac{\bar{Q}}{cn}, \qquad F = \frac{q}{cn}, \tag{4.6}$$

we find that (4.5) reduces to

$$\Theta = F + 1, \tag{4.7}$$

where

$$F = \int_0^h \frac{\partial \Psi}{\partial y} dy = \Psi(h) - \Psi(0). \tag{4.8}$$

If we choose the zero value of the streamline along the center line ($y = 0$)

$$\Psi(0) = 0, \tag{4.9}$$

then the shape of the wave is given by the streamline of value

$$\Psi(h) = F. \tag{4.10}$$

The boundary conditions for the dimensionless stream function in the moving frame are

$$\begin{aligned} \Psi &= 0 \quad \text{(by convention)}, \\ \frac{\partial^2 \Psi}{\partial y^2} &= 0 \quad \text{(by symmetry)} \end{aligned} \tag{4.11}$$

on the center line $y = 0$, and

$$\begin{aligned} \frac{\partial \Psi}{\partial y} &= -1 \quad \text{(no slip condition)}, \\ \Psi &= F \end{aligned} \tag{4.12}$$

at the wall $y = h$. We also note that h represents the dimensionless form of the surface of the peristaltic wall:

$$h(x) = 1 + \Phi \sin x, \tag{4.13}$$

where

$$\Phi = \frac{b}{n} \tag{4.14}$$

is the amplitude ratio or the occlusion and $0 < \Phi < 1$.

5. Equations for large wavelength

A general solution of the dynamic equations (3.20) for arbitrary values of all parameters seems to be impossible to find. Even in the case of Newtonian fluids, all analytical solutions obtained so far by Shapiro et al. [25], and by L. M. Srivastava and V. P. Srivastava [29] are based on assumptions that one or some of the parameters are zero or small. Accordingly, we carry out our investigation on the basis that the dimensionless wave number in (3.18) is small, that is,

$$\delta \ll 1, \tag{5.1}$$

which corresponds to the long-wavelength approximation [25]. Thus, to lowest order in δ, equations (3.20) give

$$\left(\frac{\mu+\eta}{\mu}\right)\frac{\partial p}{\partial x} = \frac{\partial S_{xy}}{\partial y} + \frac{\partial^3 \Psi}{\partial y^3}, \tag{5.2}$$

$$\frac{\partial p}{\partial y} = 0, \tag{5.3}$$

$$S_{xx} - \mathcal{W}\mathrm{e}(1+a)\frac{\partial^2 \Psi}{\partial y^2} S_{xy} = 0, \tag{5.4}$$

$$\left(\frac{\eta}{\mu}\right)\frac{\partial^2 \Psi}{\partial y^2} = S_{xy} + \frac{\mathcal{W}\mathrm{e}}{2}(1-a)\frac{\partial^2 \Psi}{\partial y^2} S_{xx} - \frac{\mathcal{W}\mathrm{e}}{2}(1+a)\frac{\partial^2 \Psi}{\partial y^2} S_{yy}, \tag{5.5}$$

$$S_{yy} + \mathcal{W}\mathrm{e}(1-a)\frac{\partial^2 \Psi}{\partial y^2} S_{xy} = 0. \tag{5.6}$$

Substituting (5.4) and (5.6) into (5.5) yields

$$S_{xy} = \frac{(\eta/\mu)\left(\partial^2 \Psi/\partial y^2\right)}{1 + \mathcal{W}\mathrm{e}^2\left(1-a^2\right)\left(\partial^2 \Psi/\partial y^2\right)^2}, \tag{5.7}$$

and from (5.2), (5.3), and (5.7), we finally obtain

$$\frac{\partial^2}{\partial y^2}\left[\frac{(\eta/\mu+1)\left(\partial^2 \Psi/\partial y^2\right) + \mathcal{W}\mathrm{e}^2\left(1-a^2\right)\left(\partial^2 \Psi/\partial y^2\right)^3}{1 + \mathcal{W}\mathrm{e}^2\left(1-a^2\right)\left(\partial^2 \Psi/\partial y^2\right)^2}\right] = 0, \tag{5.8}$$

$$\left(\frac{\mu+\eta}{\mu}\right)\frac{\partial p}{\partial x} = \frac{\partial}{\partial y}\left[\frac{(\eta/\mu)\left(\partial^2 \Psi/\partial y^2\right)}{1 + \mathcal{W}\mathrm{e}^2\left(1-a^2\right)\left(\partial^2 \Psi/\partial y^2\right)^2}\right] + \frac{\partial^3 \Psi}{\partial y^3}. \tag{5.9}$$

6. Perturbation solution

For small values of $\mathcal{W}\mathrm{e}^2$, (5.8) and (5.9) can be written using the binomial theorem as

$$\begin{aligned}
&\frac{\partial^2}{\partial y^2}\left[\frac{\partial^2 \Psi}{\partial y^2} + \mathcal{W}\mathrm{e}^2 \alpha_1 \left(\frac{\partial^2 \Psi}{\partial y^2}\right)^3 + \mathcal{W}\mathrm{e}^4 \alpha_2 \left(\frac{\partial^2 \Psi}{\partial y^2}\right)^5\right] = 0,\\
&\frac{\partial p}{\partial x} = \frac{\partial^3 \Psi}{\partial y^3} + \mathcal{W}\mathrm{e}^2 \alpha_1 \frac{\partial}{\partial y}\left[\left(\frac{\partial^2 \Psi}{\partial y^2}\right)^3\right] + \mathcal{W}\mathrm{e}^4 \alpha_2 \frac{\partial}{\partial y}\left[\left(\frac{\partial^2 \Psi}{\partial y^2}\right)^5\right],
\end{aligned} \tag{6.1}$$

where the dimensionless parameters α_1 and α_2 are defined as

$$\alpha_1 = \frac{(a^2-1)\eta}{(\eta+\mu)}, \qquad \alpha_2 = \frac{(a^2-1)^2\eta}{(\eta+\mu)}. \tag{6.2}$$

Now, we seek the solution of (6.1) with boundary conditions (4.11) and (4.12) for a small Weissenberg number. We may expand flow quantities in a power series of $\mathcal{W}\mathrm{e}^2$. We write the stream function Ψ, the pressure field p, and the flow rate F in the following forms:

$$\begin{aligned} \Psi &= \Psi_0 + \mathcal{W}\mathrm{e}^2\,\Psi_1 + \mathcal{W}\mathrm{e}^4\,\Psi_2 + \cdots, \\ p &= p_0 + \mathcal{W}\mathrm{e}^2\,p_1 + \mathcal{W}\mathrm{e}^4\,p_2 + \cdots, \\ F &= F_0 + \mathcal{W}\mathrm{e}^2\,F_1 + \mathcal{W}\mathrm{e}^4\,F_2 + \cdots. \end{aligned} \tag{6.3}$$

If we substitute (6.3) into (4.11), (4.12), (5.3), and (6.1), and separate the terms of different orders in $\mathcal{W}\mathrm{e}^2$, we obtain the following systems of partial differential equations for the stream function and pressure gradients together with boundary conditions.

6.1. System of order $\mathcal{W}\mathrm{e}^0$. The following system of equations of zeroth order follows:

$$\frac{\partial^4\Psi_0}{\partial y^4} = 0, \qquad \frac{\partial p_0}{\partial x} = \frac{\partial^3\Psi_0}{\partial y^3}, \qquad \frac{\partial p_0}{\partial y} = 0, \tag{6.4}$$

with the boundary conditions

$$\begin{aligned} &\Psi_0 = 0, \qquad \frac{\partial^2\Psi_0}{\partial y^2} = 0 \quad \text{at } y = 0, \\ &\Psi_0 = F_0, \qquad \frac{\partial\Psi_0}{\partial y} = -1 \quad \text{at } y = h. \end{aligned} \tag{6.5}$$

This boundary value problem is that of linear viscous creeping flow in the long-wavelength approximation. No properties of the Johnson-Segalman fluid enter its formulation.

6.2. System of order $\mathcal{W}\mathrm{e}^2$. The first-order differential equations are

$$\begin{aligned} \frac{\partial^4\Psi_1}{\partial y^4} &= -\alpha_1\frac{\partial^2}{\partial y^2}\left[\left(\frac{\partial^2\Psi_0}{\partial y^2}\right)^3\right], \\ \frac{\partial p_1}{\partial x} &= \frac{\partial^3\Psi_1}{\partial y^3} + \alpha_1\frac{\partial}{\partial y}\left[\left(\frac{\partial^2\Psi_0}{\partial y^2}\right)^3\right], \\ \frac{\partial p_1}{\partial y} &= 0, \end{aligned} \tag{6.6}$$

with the boundary conditions

$$\begin{aligned} \Psi_1 &= 0, \qquad \frac{\partial^2 \Psi_1}{\partial y^2} = 0 \quad \text{at } y = 0, \\ \Psi_1 &= F_1, \qquad \frac{\partial \Psi_1}{\partial y} = 0 \quad \text{at } y = h. \end{aligned} \tag{6.7}$$

At this level, the material properties—manifested via a and η—now affect the flow inside the fluid layer.

6.3. System of order $\mathcal{W}e^4$. The system of equations of the second order is composed of

$$\begin{aligned} \frac{\partial^4 \Psi_2}{\partial y^4} &= -3\alpha_1 \frac{\partial^2}{\partial y^2}\left[\left(\frac{\partial^2 \Psi_0}{\partial y^2}\right)^2 \frac{\partial^2 \Psi_1}{\partial y^2}\right] - \alpha_2 \frac{\partial^2}{\partial y^2}\left[\left(\frac{\partial^2 \Psi_0}{\partial y^2}\right)^5\right], \\ \frac{\partial p_2}{\partial x} &= \frac{\partial^3 \Psi_2}{\partial y^3} + 3\alpha_1 \frac{\partial}{\partial y}\left[\left(\frac{\partial^2 \Psi_0}{\partial y^2}\right)^2 \frac{\partial^2 \Psi_1}{\partial y^2}\right] + \alpha_2 \frac{\partial}{\partial y}\left[\left(\frac{\partial^2 \Psi_0}{\partial y^2}\right)^5\right], \\ \frac{\partial p_2}{\partial y} &= 0, \end{aligned} \tag{6.8}$$

with the boundary conditions

$$\begin{aligned} \Psi_2 &= 0, \qquad \frac{\partial^2 \Psi_2}{\partial y^2} = 0 \quad \text{at } y = 0, \\ \Psi_2 &= F_2, \qquad \frac{\partial \Psi_2}{\partial y} = 0 \quad \text{at } y = h. \end{aligned} \tag{6.9}$$

In this system, further corrections due to the Johnson-Segalman constitutive equation enter. We now seek to solve the sequence of problems at each order and generate thereby the series solution.

6.4. Zeroth-order solution. The solution to the zeroth-order problem (6.4) subject to the boundary conditions (6.5) is given by

$$\begin{aligned} \Psi_0 &= -\frac{3}{2}(F_0 + h)\left[\frac{y^3}{3h^3} - \frac{y}{h}\right] - y, \\ u_0 &= -\frac{3}{2h}(F_0 + h)\left[\frac{y^2}{h^2} - 1\right] - 1. \end{aligned} \tag{6.10}$$

From the second and third equations in (6.4), it is clear that the transverse pressure gradient is zero and the longitudinal pressure gradient is given by

$$\frac{dp_0}{dx} = -3\left(\frac{F_0}{h^3} + \frac{1}{h^2}\right). \tag{6.11}$$

The pressure rise per wavelength ($\triangle P_\lambda$) in the longitudinal direction can be evaluated on the axis at $y = 0$. Thus, at the zeroth order, we have

$$\triangle P_{\lambda_0} = \int_0^{2\pi} \frac{dp_0}{dx} dx = -3[I_3 F_0 + I_2], \tag{6.12}$$

where

$$I_2 = \frac{2\pi}{(1-\Phi^2)^{3/2}}, \qquad I_3 = \frac{\pi(2+\Phi^2)}{(1-\Phi^2)^{5/2}}. \tag{6.13}$$

The expressions (6.10), (6.11), and (6.12) are essentially the same as those of the Newtonian fluid given by Shapiro et al. [25]. This is obviously no surprise.

6.5. First-order solution ($\mathbb{O}(\mathbb{W}e^2)$)**.** Substituting the zeroth-order solution into (6.6), the system of order $\mathbb{W}e^2$ reduces the latter to

$$\begin{aligned} \frac{\partial^4 \Psi_1}{\partial y^4} &= -\alpha_1 \frac{\partial^2}{\partial y^2}\left[y^3 \left(\frac{dp_0}{dx}\right)^3 \right], \\ \frac{dp_1}{dx} &= \frac{\partial^3 \Psi_1}{\partial y^3} + \alpha_1 \frac{\partial}{\partial y}\left[y^3 \left(\frac{dp_0}{dx}\right)^3 \right]. \end{aligned} \tag{6.14}$$

On solving (6.14) with boundary conditions (6.7), the expressions for the stream function Ψ_1, the axial velocity component u_1, the longitudinal pressure gradient dp_1/dx, and the pressure rise per wavelength $\triangle P_{\lambda_1}$ turn out to be

$$\begin{aligned} \Psi_1 &= \frac{\alpha_1}{2}\left(\frac{dp_0}{dx}\right)^3 \left[-\frac{y^5}{10} + \frac{h^2 y^3}{5} - \frac{h^4 y}{10} \right] - \frac{3F_1}{2}\left[\frac{y^3}{3h^3} - \frac{y}{h} \right], \\ u_1 &= \frac{\alpha_1}{2}\left(\frac{dp_0}{dx}\right)^3 \left[-\frac{y^4}{2} + \frac{3h^2 y^2}{5} - \frac{h^4}{10} \right] - \frac{3F_1}{2h}\left[\frac{y^2}{h^2} - 1 \right], \\ \frac{dp_1}{dx} &= \frac{\alpha_1}{2}\left(\frac{dp_0}{dx}\right)^3 \left[\frac{6h^2}{5} \right] - \frac{3F_1}{h^3}, \\ \triangle P_{\lambda_1} &= -\frac{81\alpha_1}{5}[I_7 F_0^3 + 3I_6 F_0^2 + 3I_5 F_0 + I_4] - 3F_1 I_3, \end{aligned} \tag{6.15}$$

where

$$\begin{aligned} I_4 &= \frac{\pi(3\Phi^2+2)}{(1-\Phi^2)^{7/2}}, \\ I_n &= \int_0^{2\pi} \frac{1}{h^n} dx = \frac{1}{(1-\Phi^2)}\left[\left(\frac{2n-3}{n-1}\right) I_{n-1} - \left(\frac{n-2}{n-1}\right) I_{n-2} \right], \quad n > 4. \end{aligned} \tag{6.16}$$

6.6. Second-order solution ($\mathbb{O}(\mathbb{W}e^4)$)**.** If we insert the zeroth-order and first-order solutions into (6.8), we find that the system of $\mathbb{O}(\mathbb{W}e^4)$ takes the form

$$\begin{aligned}
\frac{\partial^4\Psi_2}{\partial y^4} &= -3\alpha_1\frac{\partial^2}{\partial y^2}\left[\frac{\alpha_1}{2}\left(\frac{dp_0}{dx}\right)^5\left(-2y^5+\frac{6}{5}h^2y^3\right)-\left(\frac{dp_0}{dx}\right)^2\left(\frac{3F_1y^3}{h^3}\right)\right]\\
&\quad-\alpha_2\frac{\partial^2}{\partial y^2}\left[y^5\left(\frac{dp_0}{dx}\right)^5\right],\\
\frac{dp_2}{dx} &= \frac{\partial^3\Psi_2}{\partial y^3}+3\alpha_1\frac{\partial}{\partial y}\left[\frac{\alpha_1}{2}\left(\frac{dp_0}{dx}\right)^5\left(-2y^5+\frac{6}{5}h^2y^3\right)-\left(\frac{dp_0}{dx}\right)^2\left(\frac{3F_1y^3}{h^3}\right)\right]\\
&\quad+\alpha_2\frac{\partial}{\partial y}\left[y^5\left(\frac{dp_0}{dx}\right)^5\right].
\end{aligned}\tag{6.17}$$

Solving (6.17), subject to the boundary conditions (6.9), we find, after lengthy calculations, that

$$\begin{aligned}
\Psi_2 &= \frac{3\alpha_1^2}{2}\left(\frac{dp_0}{dx}\right)^5\left[\frac{y^7}{21}-\frac{3y^5h^2}{50}-\frac{4y^3h^4}{175}+\frac{74yh^6}{2100}\right]\\
&\quad+\frac{3\alpha_1}{2}\left(\frac{dp_0}{dx}\right)^2\frac{F_1}{h^3}\left[\frac{3y^5}{10}-\frac{3y^3h^2}{5}+\frac{3yh^4}{10}\right]\\
&\quad-\alpha_2\left(\frac{dp_0}{dx}\right)^5\left[\frac{y^7}{42}-\frac{y^3h^4}{14}+\frac{yh^6}{21}\right]+\frac{3F_2}{2}\left[\frac{y}{h}-\frac{y^3}{3h^3}\right],
\end{aligned}\tag{6.18}$$

$$\begin{aligned}
u_2 &= \frac{3\alpha_1^2}{2}\left(\frac{dp_0}{dx}\right)^5\left[\frac{y^6}{3}-\frac{3y^4h^2}{10}-\frac{12y^2h^4}{175}+\frac{74h^6}{2100}\right]\\
&\quad+\frac{3\alpha_1}{2}\left(\frac{dp_0}{dx}\right)^2\frac{F_1}{h^3}\left[\frac{3y^4}{2}-\frac{9y^2h^2}{5}+\frac{3h^4}{10}\right]\\
&\quad-\alpha_2\left(\frac{dp_0}{dx}\right)^5\left[\frac{y^6}{6}-\frac{3y^2h^4}{14}+\frac{h^6}{21}\right]+\frac{3F_2}{2h}\left[1-\frac{y^2}{h^2}\right],
\end{aligned}\tag{6.19}$$

$$\begin{aligned}
\frac{dp_2}{dx} &= -\frac{3\alpha_1^2}{2}\left(\frac{dp_0}{dx}\right)^5\left[\frac{24h^4}{175}\right]-\frac{3\alpha_1}{2}\left(\frac{dp_0}{dx}\right)^2\left[\frac{18F_1}{5h}\right]\\
&\quad+\frac{3h^4\alpha_2}{7}\left(\frac{dp_0}{dx}\right)^5-\frac{3F_2}{h^3}.
\end{aligned}\tag{6.20}$$

The pressure rise per wavelength in the longitudinal direction can be obtained by substituting (6.11) in (6.20) and integrating the resulting equation with respect to x from 0 to 2π. The result is given by

$$\begin{aligned}
\triangle P_{\lambda_2} &= \left(\frac{8748}{175}\alpha_1^2-\frac{729}{7}\alpha_2\right)\left[I_{11}F_0^5+5I_{10}F_0^4+10I_9F_0^3+10I_8F_0^2+5F_0I_7+I_6\right]\\
&\quad-\frac{243}{5}\alpha_1F_1\left[I_7F_0^2+2I_6F_0+I_5\right]-3F_2I_3,
\end{aligned}\tag{6.21}$$

where I_n is given by (6.16).

Now we summarize our results of the perturbation series through order $\mathcal{We}^4$. The expressions for Ψ, u, dp/dx, and $\triangle P_\lambda$ may, respectively, take the following forms:

$$\begin{aligned}
\Psi = {} & \left[-\frac{3}{2}(F_0+h)\left(\frac{y^3}{3h^3}-\frac{y}{h}\right)-y\right] \\
& +\mathcal{We}^2\left[\frac{\alpha_1}{2}\left(\frac{dp_0}{dx}\right)^3\left(-\frac{y^5}{10}+\frac{h^2y^3}{5}-\frac{h^4y}{10}\right)-\frac{3F_1}{2}\left(\frac{y^3}{3h^3}-\frac{y}{h}\right)\right] \\
& +\mathcal{We}^4\left[\frac{3\alpha_1^2}{2}\left(\frac{dp_0}{dx}\right)^5\left(\frac{y^7}{21}-\frac{3y^5h^2}{50}-\frac{4y^3h^4}{175}+\frac{74yh^6}{2100}\right)\right. \\
& \quad +\frac{3\alpha_1}{2}\left(\frac{dp_0}{dx}\right)^2\frac{F_1}{h^3}\left(\frac{3y^5}{10}-\frac{3y^3h^2}{5}+\frac{3yh^4}{10}\right) \\
& \quad \left.-\alpha_2\left(\frac{dp_0}{dx}\right)^5\left(\frac{y^7}{42}-\frac{y^3h^4}{14}+\frac{yh^6}{21}\right)+\frac{3F_2}{2}\left(\frac{y}{h}-\frac{y^3}{3h^3}\right)\right],
\end{aligned} \tag{6.22}$$

$$\begin{aligned}
u = {} & \left[-\frac{3}{2h}(F_0+h)\left(\frac{y^2}{h^2}-1\right)-1\right] \\
& +\mathcal{We}^2\left[\frac{\alpha_1}{2}\left(\frac{dp_0}{dx}\right)^3\left(-\frac{y^4}{2}+\frac{3h^2y^2}{5}-\frac{h^4}{10}\right)-\frac{3F_1}{2h}\left(\frac{y^2}{h^2}-1\right)\right] \\
& +\mathcal{We}^4\left[\frac{3\alpha_1^2}{2}\left(\frac{dp_0}{dx}\right)^5\left(\frac{y^6}{3}-\frac{3y^4h^2}{10}-\frac{12y^2h^4}{175}+\frac{74h^6}{2100}\right)\right. \\
& \quad +\frac{3\alpha_1}{2}\left(\frac{dp_0}{dx}\right)^2\frac{F_1}{h^3}\left(\frac{3y^4}{2}-\frac{9y^2h^2}{5}+\frac{3h^4}{10}\right) \\
& \quad \left.-\alpha_2\left(\frac{dp_0}{dx}\right)^5\left(\frac{y^6}{6}-\frac{3y^2h^4}{14}+\frac{h^6}{21}\right)+\frac{3F_2}{2h}\left(1-\frac{y^2}{h^2}\right)\right],
\end{aligned} \tag{6.23}$$

$$\begin{aligned}
\frac{dp}{dx} = {} & \frac{dp_0}{dx}+\mathcal{We}^2\left[\frac{\alpha_1}{2}\left(\frac{dp_0}{dx}\right)^3\left(\frac{6h^2}{5}\right)-\frac{3F_1}{h^3}\right] \\
& +\mathcal{We}^4\left[-\frac{3\alpha_1^2}{2}\left(\frac{dp_0}{dx}\right)^5\left(\frac{24h^4}{175}\right)-\frac{3\alpha_1}{2}\left(\frac{dp_0}{dx}\right)^2\left(\frac{18F_1}{5h}\right)\right. \\
& \quad \left.+\frac{3h^4\alpha_2}{7}\left(\frac{dp_0}{dx}\right)^5-\frac{3F_2}{h^3}\right],
\end{aligned} \tag{6.24}$$

$$\begin{aligned}
\triangle P_\lambda = {} & -3\left[I_3F_0+I_2\right] \\
& +\mathcal{We}^2\left[-\frac{81\alpha_1}{5}\left[I_7F_0^3+3I_6F_0^2+3I_5F_0+I_4\right]-3F_1I_3\right] \\
& +\mathcal{We}^4\left[\left(\frac{8748}{175}\alpha_1^2-\frac{729}{7}\alpha_2\right)\right. \\
& \quad \times\left(I_{11}F_0^5+5I_{10}F_0^4+10I_9F_0^3+10I_8F_0^2+5I_7F_0+I_6\right) \\
& \quad \left.-\frac{243}{5}\alpha_1F_1\left[I_7F_0^2+2I_6F_0+I_5\right]-3F_2I_3\right].
\end{aligned} \tag{6.25}$$

If we define

$$F^{(2)} = F_0 + \mathcal{W}\mathrm{e}^2 F_1 + \mathcal{W}\mathrm{e}^4 F_2, \tag{6.26}$$

then

$$\begin{aligned} F_0 &= F^{(2)} - \mathcal{W}\mathrm{e}^2 F_1 - \mathcal{W}\mathrm{e}^4 F_2, \\ \mathcal{W}\mathrm{e}^2 F_1 &= F^{(2)} - F_0 - \mathcal{W}\mathrm{e}^4 F_2, \\ \mathcal{W}\mathrm{e}^4 F_2 &= F^{(2)} - F_0 - \mathcal{W}\mathrm{e}^2 F_1. \end{aligned} \tag{6.27}$$

On substituting these expressions into (6.25) and retaining only terms up to order $\mathcal{W}\mathrm{e}^4$, we obtain

$$\begin{aligned} \triangle P_\lambda^{(2)} = {} & -3\left[I_3 F^{(2)} + I_2\right] \\ & + \mathcal{W}\mathrm{e}^2 \left[-\frac{81\alpha_1}{5}\left(I_7 \left(F^{(2)}\right)^3 + 3I_6 \left(F^{(2)}\right)^2 + 3F^{(2)} I_5 + I_4\right)\right] \\ & + \mathcal{W}\mathrm{e}^4 \left[\left(\frac{8748}{175}\alpha_1^2 - \frac{729}{7}\alpha_2\right)\left(I_6 + 5F^{(2)} I_7 + 10\left(F^{(2)}\right)^2 I_8 + 10\left(F^{(2)}\right)^3 I_9 \right.\right. \\ & \qquad \left.\left. + 5\left(F^{(2)}\right)^4 I_{10} + \left(F^{(2)}\right)^5 I_{11}\right)\right]. \end{aligned} \tag{6.28}$$

7. Numerical method

We will solve the differential equation (5.8) with the boundary conditions (4.11) and (4.12). Its approximate solution for small values of $\mathcal{W}\mathrm{e}^2$ has been obtained in the previous section and is demonstrated in (6.22). Its solution for any large value of $\mathcal{W}\mathrm{e}^2$ can be obtained by numerical methods.

This two-point boundary value problem can be rewritten as

$$\frac{\partial^2}{\partial y^2}\left[\frac{(\eta/\mu)\left(\partial^2\Psi/\partial y^2\right)}{1 + \mathcal{W}\mathrm{e}^2\left(1-a^2\right)\left(\partial^2\Psi/\partial y^2\right)^2}\right] + \frac{\partial^4\Psi}{\partial y^4} = 0 \tag{7.1}$$

with the boundary conditions

$$\begin{aligned} \Psi &= 0, \qquad \frac{\partial^2\Psi}{\partial y^2} = 0 \quad \text{at } y = 0, \\ \Psi &= F, \qquad \frac{\partial\Psi}{\partial y} = -1 \quad \text{at } y = h. \end{aligned} \tag{7.2}$$

Because the differential equation (7.1) is nonlinear, we cannot solve this boundary value problem by the direct finite-difference method. In fact, in solving such nonlinear equations, iterative methods are usually used, and one of them is the asymptotic method.

A general stationary problem

$$f\left(\Psi(y), y\right) = 0, \quad y \in (a, b), \tag{7.3}$$

accompanied with suitable boundary conditions, in which f may be a nonlinear higher-order differential function, can be treated as the steady asymptotic limit as $t \to \infty$ of the nonstationary problem

$$\frac{\partial \phi}{\partial t} + f\left(\phi(y,t), y\right) = 0. \tag{7.4}$$

It follows that

$$\lim_{t\to\infty} \phi(y,t) = \Psi(y). \tag{7.5}$$

In solving the stationary problem (7.3) by asymptotic methods, that is, in solving the nonstationary problem (7.4), we do not pay any attention to the transient behavior since it is of no interest whatsoever.

Clearly, the nonstationary problem for ϕ, (7.4), can be solved by using finite-difference methods with respect to t. For example,

$$\frac{\phi^{n+1} - \phi^n}{\tau} + f\left(\phi^n, y\right) = 0 \tag{7.6}$$

or

$$\phi^{n+1} = \phi^n - \tau f\left(\phi^n, y\right), \tag{7.7}$$

where the counting index n indicates the time step and has nothing in common with the channel width n. As for the stationary problem (7.3), the solution is given by

$$\lim_{n\to\infty} \phi^n = \Psi. \tag{7.8}$$

In any case, from the point of view of solving the stationary problem, it is convenient to interpret the index n as denoting the iteration step rather than time, and in this case the real parameter τ indicates the iteration over-relaxation factor rather than the size of the time step. The parameter τ should be, on the one hand, sufficiently small to guarantee convergent iteration, and, on the other hand, as large as possible to minimize the number of iterations.

If f is a differential function, we can obtain the discrete approximate solutions $\phi_1(y_1)$, $\phi_2(y_2), \ldots, \phi_M(y_M)$ at discrete points $a < y_1 < y_2 < \cdots < y_M < b$ by employing the difference equation

$$\phi_j^{n+1} = \phi_j^n - \tau g\left(\phi_1^n, \ldots, \phi_M^n, y_j\right), \tag{7.9}$$

in which the algebraic function g can be obtained by means of finite-difference approximations with respect to the algebra-differential function f in (7.7).

Here, we describe this method as applied to the boundary value problem (7.1) and (7.2). Instead of solving the stationary problem (7.1), we solve the nonstationary equation

$$\frac{\partial \phi}{\partial t} + \frac{\partial^2}{\partial y^2}\left[\frac{(\eta/\mu)\left(\partial^2\phi/\partial y^2\right)}{1 + \mathcal{W}\mathrm{e}^2\left(1-a^2\right)\left(\partial^2\phi/\partial y^2\right)^2}\right] + \frac{\partial^4 \phi}{\partial y^4} = 0, \tag{7.10}$$

whose finite-difference form is

$$\frac{\phi_j^{n+1}-\phi_j^n}{\tau}+\frac{1}{(\Delta y)^2}\{c_{j+1}^n-2c_j^n+c_{j-1}^n\}+\frac{1}{(\Delta y)^4}\{\phi_{j+2}^n-4\phi_{j+1}^n+6\phi_j^n-4\phi_{j-1}^n+\phi_{j-2}^n\}=0 \tag{7.11}$$

with the expression for c_j^n given by

$$c_j^n=\frac{(\eta/\mu)\left((\phi_{j+1}^n-2\phi_j^n+\phi_{j-1}^n)/(\Delta y)^2\right)}{1+\mathcal{W}\mathrm{e}\,(1-a^2)\left((\phi_{j+1}^n-2\phi_j^n+\phi_{j-1}^n)/(\Delta y)^2\right)} \tag{7.12}$$

for the iteration steps $n=0,1,2,\ldots,\infty$ and at space points $j=2,3,\ldots,M-1$ (where $y=2\Delta y,3\Delta y,\ldots,(M-1)\Delta y$) with the grid size $\Delta y=h/(M-1)$.

The boundary conditions (7.2) can be described in finite-difference forms as follows:

$$\phi_0^{n+1}=\phi_2^{n+1},\qquad \phi_1^{n+1}=0,\qquad \phi_M^{n+1}=F,\qquad \phi_{M+1}^{n+1}=\phi_{M-1}^{n+1}-2\Delta y. \tag{7.13}$$

We start with an initial trial solution ϕ_j^0 $(j=0,1,2,\ldots,m+1)$, which satisfies the boundary conditions (7.13). The iteration should be carried out until the relative differences of the computed ϕ_j^n and ϕ_j^{n+1} between two successive iterative steps for all discrete points are smaller than a given error chosen to be 10^{-8}. Therefore, the stationary solution, the solution of the stationary boundary value problem (7.1) and (7.2), is achieved.

8. Numerical results and discussions

A comparison of the direct numerical results as obtained for the boundary value problem (7.1) and (7.2) and its approximate perturbation solutions to order $\mathcal{W}\mathrm{e}^4$, (6.22) and (6.23), is shown in Figure 8.1. We display the dimensionless stream function Ψ (left panels) and the dimensionless velocity u obtained with three different values of the Weissenberg number $\mathcal{W}\mathrm{e}=0.8,1.0,1.5$ and a fixed total flux $F=-2$. It is surprising and pleasing that, for fairly large $\mathcal{W}\mathrm{e}$, for example, $\mathcal{W}\mathrm{e}=0.8$, good agreement between the approximate solutions and the direct numerical solutions can be achieved. When $\mathcal{W}\mathrm{e}=1$, and more so when $\mathcal{W}\mathrm{e}>1.0$, their difference becomes conspicuously large. In fact, such a performance can be predicted. It is dependent on the choice of the total flux F. For $F=-2$ used in Figure 8.1, the distribution of the stream function is close to linear, as we can see in Figures 8.1(a), 8.1(c), and 8.1(e). In such a case, the term with $\mathcal{W}\mathrm{e}$ in (7.1), which is proportional to the second-order spatial derivative of the stream function, cannot become important. We can demonstrate this even more clearly if we choose $F=-1$. In this case, the solution of the boundary value problem yields a rigorously linear distribution of the stream function (i.e., constant velocity), and hence its second-order spatial derivative vanishes. Therefore, the results of the approximate perturbation solutions are in accordance with those of the direct numerical solutions which hold for any value of $\mathcal{W}\mathrm{e}$.

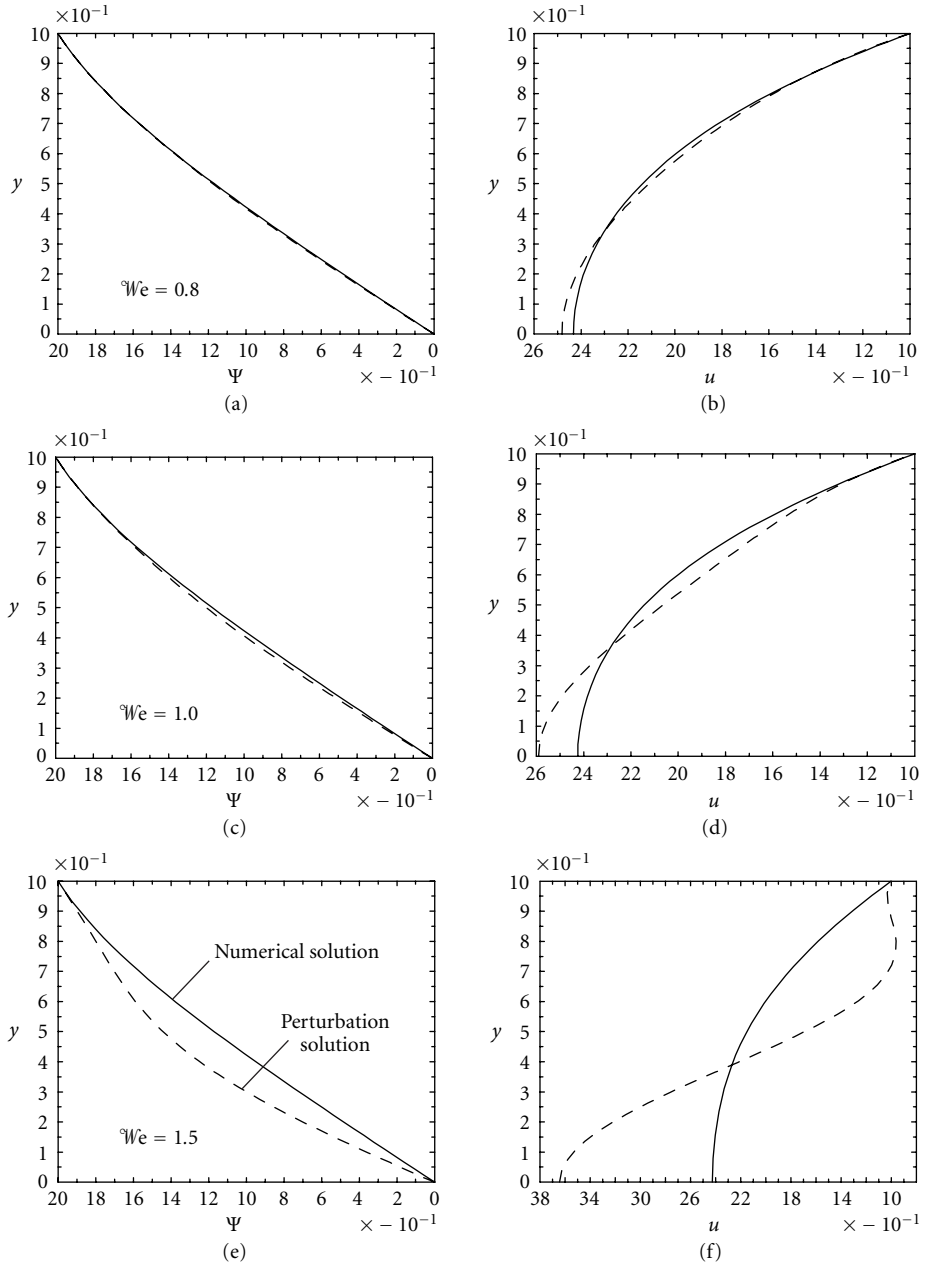

Figure 8.1. Profiles of dimensionless stream function $\Psi(y)$ (left) and velocity $u(y)$ (right). Solid lines indicate the numerical solutions of the boundary value problem (7.1) and (7.2), while dashed lines denote their approximate perturbation solutions. The Weissenberg number $\mathcal{We}$ is chosen as $\mathcal{We} = 0.8$ (Figures (a) and (b)), $\mathcal{We} = 1.0$ (Figures (c) and (d)), and $\mathcal{We} = 1.5$ (Figures (e) and (f)), respectively. The total flux is kept a fixed value of $F = -2$. The other parameters are chosen as $h = 1$, $\mu/\eta = 1$, and $a = 0.8$.

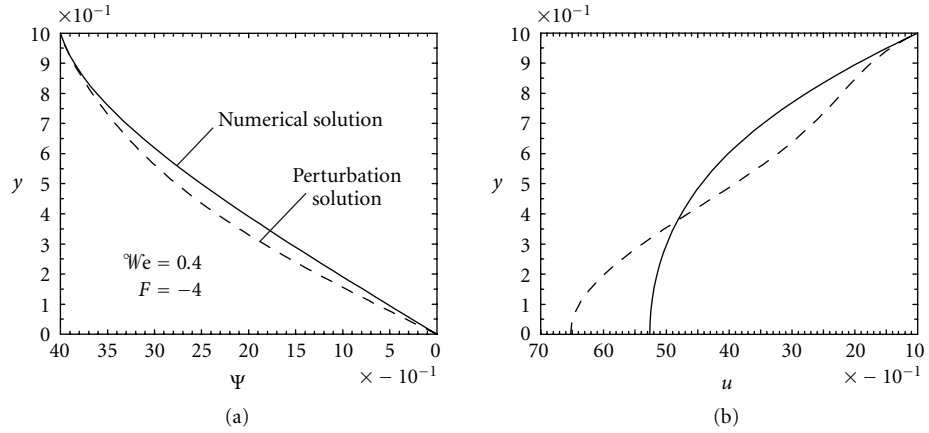

Figure 8.2. Profiles of (a) dimensionless stream function $\Psi(y)$, (b) velocity $u(y)$. Solid lines indicate the numerical solutions of the boundary value problem (7.1) and (7.2), while dashed lines denote their approximate perturbation solutions. The Weissenberg number $\mathcal{We}$ is chosen as $\mathcal{We} = 0.4$ and the total flux is kept a fixed value of $F = -4$.

In fact, if we choose $F = -4$, for which a larger deviation of the stream function from the linear distribution is obtained, an obvious difference of the approximate perturbation solutions from the direct numerical solutions can be seen, although $\mathcal{We}$ takes a fairly small value $\mathcal{We} = 0.4$, as displayed in Figure 8.2. Only when $\mathcal{We} = 0.1$ the perturbation solution is an adequate approximation.

To quantitatively discriminate to what extent the perturbation solutions (6.22) and (6.23) can describe the boundary value problem (7.1) and (7.2), an error measure for a physical variable φ, for example, the stream function Ψ and the velocity u, is introduced:

$$\mathscr{E}_{\varphi} = \sqrt{\frac{\sum_j \left(\varphi_j^{\text{app}} - \varphi_j^{\text{num}}\right)^2}{\sum_j \left(\varphi_j^{\text{num}}\right)^2}}, \tag{8.1}$$

where φ_j^{num} denotes the direct numerical solution at the space position y_j, while φ_j^{app} is the corresponding approximate value obtained by the perturbation solutions (6.22) and (6.23).

For various Weissenberg numbers $\mathcal{We}$, the errors of the two solutions are listed in Table 8.1 with two different values of the total flux F. It is obvious that the errors increase with the increasing Weissenberg number $\mathcal{We}$. For $F = -2$, if $\mathcal{We} > 0.8$, the approximate solutions can no longer be used, while for a larger total flux value $F = -4$, the approximate perturbation solutions have to be abandoned for as small values as $\mathcal{We} > 0.2$. In such cases, this boundary value problem must be solved by direct numerical methods.

In Figure 8.3 the distributions of the stream function $\Psi(y)$ and the velocity $u(y)$ are illustrated for various values of the total flux F. Results are obtained by the direct numerical method because here we choose a large value of $\mathcal{We} = 1.5$ and hence the perturbation

Table 8.1. Errors percentages for the stream function Ψ and the velocity u between the numerical solutions and the approximate perturbation solutions of the boundary value problem (7.1) and (7.2) listed for different Weissenberg numbers $\mathcal{We}$ and fluxes F.

	$\mathcal{We}$	0.0	0.2	0.4	0.6	0.8	1.0	1.2	1.5	2.0
$F=-2$	$\mathcal{E}_\Psi$	0.06	0.06	0.08	0.12	0.48	1.84	4.93	15.0	56.4
	$\mathcal{E}_u$	0.02	0.02	0.03	0.27	1.31	4.47	11.4	33.8	124.9
$F=-4$	$\mathcal{E}_\Psi$	0.10	0.11	7.1	50.5	179.6	462.3	—	—	—
	$\mathcal{E}_u$	0.21	0.39	16.8	144.4	402.8	1033.2	—	—	—

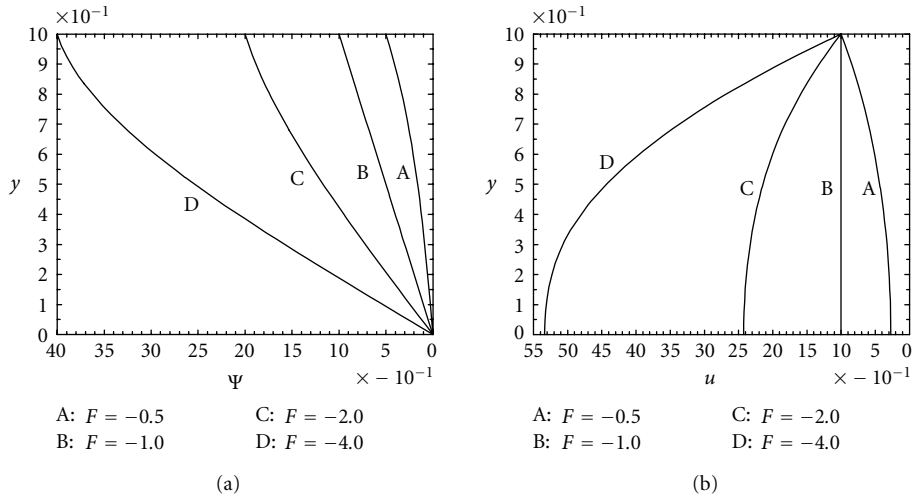

Figure 8.3. Profiles of (a) dimensionless stream function $\Psi(y)$, (b) velocity $u(y)$ simulated for various values of the total flux $F=-0.5,-1.0,-2.0$, and -4.0, respectively. The other parameters are $h=1$, $\mu/\eta=1$, $a=0.8$, and $\mathcal{We}=1.5$.

solutions are no valid approximation. Obviously, the flow is dominantly influenced by the value of F. For a half-channel width of $h=1$, if $F>1$, the flow velocity near the channel center is larger than that at the top boundary due to an exerted pressure gradient in the direction opposite to the flow, while for $F<1$, a pressure gradient in the flow direction is required to maintain such a flux value, hence the flow velocity near the channel center is smaller. For $F=1$, a linear distribution of the stream function and a constant velocity are formed; in this case, no pressure gradient exists.

The distributions of the pressure gradient dp/dx within a wavelength $x\in[0,2\pi]$ are exhibited in Figure 8.4 for various values of the dimensionless wave amplitude Φ (Figure 8.4(a)) and the total flux F (Figure 8.4(b)). The dimensionless half-channel width is defined by (4.13), that is, $h(x)=1+\Phi\sin x$. The results are plotted for the approximate perturbation expression (6.24) because we here choose a small value of $\mathcal{We}=0.2$, and hence an adequate approximation by the perturbation method can still be ensured. For a

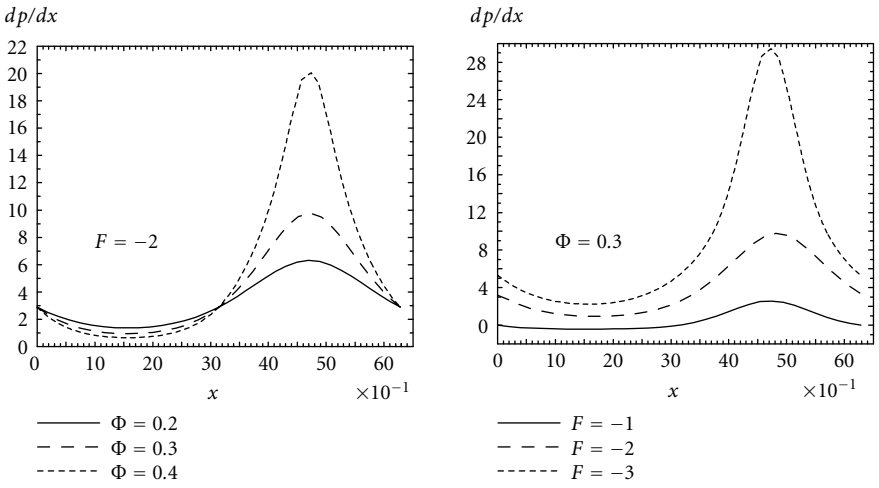

Figure 8.4. Distributions of the pressure gradient dp/dx within a wavelength $x \in [0, 2\pi]$ for different values of the amplitude ratio Φ (Figure (a)) and the total flux F (Figure (b)). The other parameters are $\mu/\eta = 1$, $a = 0.8$, and $\mathcal{We} = 0.2$.

Table 8.2. Pressure drop per wavelength in the longitudinal direction for various values of the total flux F and the wave amplitude Φ. The other parameters are $\mu/\eta = 1$, $a = 0.8$, and $\mathcal{We} = 0.2$.

F	-0.5			-1.0			-2.0			-3.0		
Φ	0.2	0.3	0.4	0.2	0.3	0.4	0.2	0.3	0.4	0.2	0.3	0.4
$\triangle P_\lambda$	−9.31	−9.17	−8.68	1.25	3.18	6.77	21.1	25.4	36.2	39.3	57.8	166.7

larger $\mathcal{We}$, one has to directly solve the boundary value problem (7.1) and (7.2) for various values of the channel width h within a wavelength and then substitute the results into (5.9) in order to obtain the pressure gradient at various points along the channel.

It can be clearly seen from Figure 8.4 that, on the one hand, in the wide part of the channel, $x \in [0, \pi]$, the pressure gradient is relatively small, that is, the flow can easily pass without imposition of a large pressure gradient. On the other hand, in a narrow part of the channel, $x \in [\pi, 2\pi]$, a much larger pressure gradient is required to maintain the same flux to pass it, especially for the narrowest position near $x = 3\pi/2$ and when the flux F or the wave amplitude Φ is larger.

The corresponding pressure drops in the flow direction over a wavelength are listed in Table 8.2 for some values of F and Φ. These are still obtained by the perturbation method, that is, (6.25) due to the used small value of $\mathcal{We} = 0.2$. For small values of F, a pressure rise occurs in the flow direction. With the increase of the flux F and the wave amplitude Φ, the pressure drops increase over a wavelength.

9. Conclusions

Plane steady peristaltic motions of a Johnson-Segalman fluid were analyzed for the conditions that the wall surface is sinusoidally deformed. This wall deformation has wavelength λ which is large in comparison to the undeformed channel width and propagates at a prescribed constant speed. The time-independent governing equations of this boundary value problem are expressed in terms of the stream function and pressure as basic unknowns with wall boundary conditions formulated in terms of the stream function alone. By prescribing the constant value of this stream function of the wall, the flux caused by the peristaltic wall deformation is prescribed. A scale analysis and associated nondimensionalization of the equations paired with a Galilee-transformation with speed c discloses a steady time-independent problem in which an aspect ratio parameter δ and the Weissenberg number $\mathcal{W}\mathrm{e}$ appear as the significant physical scales. The equations in the limit $\delta \to 0$ describe the large-wavelength approximation. These equations still contain the Weissenberg number $\mathcal{W}\mathrm{e}$ as a parameter. Perturbation solutions up to $\mathbb{O}(\mathcal{W}\mathrm{e}^4)$ for the flow have been constructed for prescribed flux F and these solutions have been compared with numerical solutions that are valid for any value of the Weissenberg number. The following results are found.

(i) The deviation of the flow from a linear stream function and a constant velocity depends on both the flux F as well as the Weissenberg number $\mathcal{W}\mathrm{e}$. For $F = -1$, the viscoelastic properties do not enter the flow no matter how large $\mathcal{W}\mathrm{e}$ is.

(ii) With growing $|F|$ (decreasing F to large negative values) the influence of the viscoelastic properties of the fluid becomes more and more significant.

(iii) The profiles of the stream functions and the longitudinal velocities as computed with the perturbation expansion are only adequately predicted when the Weissenberg number $\mathcal{W}\mathrm{e}$ is small. The maximum values for which the perturbation solutions are valid approximations depend on the flux variable F. It is the smaller, the larger the deviation F from -1 is.

(iv) In general, the solutions ought to be numerically determined by using the full equations valid for all $\mathcal{W}\mathrm{e}$.

(v) The pressure that develops for a certain flux depends very much on the flux parameter. Generally, rather localized maxima can arise (Figure 8.4). Such maxima can be controlled by adequately choosing the flux.

The next analysis will obviously be the corresponding peristaltic motion of a fluid in a circular flexible duct. This problem is presently under analysis.

Acknowledgment

T. Hayat thanks the Alexander von Humboldt Foundation for financial support.

References

[1] K. Ayukawa, T. Kawa, and M. Kimura, *Streamlines and pathlines in peristaltic flows at high Reynolds numbers*, Bull. Japan Soc. Mech. Engrs. **24** (1981), 948–955.

[2] G. Böhme and R. Friedrich, *Peristaltic flow of viscoelastic liquids*, J. Fluid Mech. **128** (1983), 109–122.

[3] T. D. Brown and T.-K. Hung, *Computational and experimental investigations of two-dimensional nonlinear peristaltic flows*, J. Fluid Mech. **83** (1977), 249–272.
[4] J. C. Burns and T. Parkes, *Peristaltic motion*, J. Fluid Mech. **29** (1967), 731–743.
[5] T. S. Chow, *Peristaltic transport in a circular cylindrical pipe*, J. Appl. Mech. **37** (1970), 901–905.
[6] Y. C. Fung and C. S. Yih, *Peristaltic transport*, J. Appl. Mech. **35** (1968), 669–675.
[7] S. K. Guha, H. Kaur, and A. M. Ahmad, *Mechanism of spermatic flow in the vas deference*, Med. Biol. Eng. **13** (1975), 518–522.
[8] M. Hanin, *The flow through a channel due to transversely oscillating walls*, Israel J. Tech. **6** (1968), 67–71.
[9] M. W. Johnson Jr. and D. Segalman, *A model for viscoelastic fluid behavior which allows non-affine deformation*, J. non-Newtonian Fluid Mech. **2** (1977), 255–270.
[10] R. W. Kolkka, D. S. Malkus, M. G. Hansen, G. R. Ierly, and R. A. Worthing, *Spurt phenomenon of the Johnson-Segalman fluid and related models*, J. non-Newtonian Fluid Mech. **29** (1988), 303–335.
[11] A. M. Kraynik and W. R. Schowalter, *Slip at the wall and extrudate roughness with aqueous solutions of polyvinyl alcohol and sodium borate*, J. Rheol. **25** (1981), no. 1, 95–114.
[12] F. J. Lim and W. R. Schowalter, *Wall slip of narrow molecular weight distribution polybutadienes*, J. Rheol. **33** (1989), no. 8, 1359–1382.
[13] D. S. Malkus, J. A. Nohel, and B. J. Plohr, *Dynamics of shear flow of a non-Newtonian fluid*, J. Comput. Phys. **87** (1990), no. 2, 464–487.
[14] ———, *Analysis of new phenomena in shear flow of non-Newtonian fluids*, SIAM J. Appl. Math. **51** (1991), no. 4, 899–929.
[15] T. C. B. McLeish and R. C. Ball, *A molecular approach to the spurt effect in polymer melt flow*, J. Polym. Sci. (B) **24** (1986), 1735–1745.
[16] K. B. Migler, H. Hervert, and L. Leger, *Slip transition of a polymer melt under shear stress*, Phys. Rev. Lett. **70** (1990), no. 3, 287–290.
[17] K. B. Migler, G. Massey, H. Hervert, and L. Leger, *The slip transition at the polymer-solid interface*, J. Phys. Condens. Matter **6** (1994), A301–A304.
[18] J. C. Misra and S. K. Pandey, *Peristaltic transport in a tapered tube*, Math. Comput. Modelling **22** (1995), no. 8, 137–151.
[19] ———, *Peristaltic transport of a non-Newtonian fluid with a peripheral layer*, Internat. J. Engrg. Sci. **37** (1999), 1841–1858.
[20] K. K. Raju and R. Devanathan, *Peristaltic motion of a non-Newtonian fluid*, Rheol. Acta **11** (1972), 170–178.
[21] ———, *Peristaltic motion of a non-Newtonian fluid. II: visco-elastic fluid*, Rheol. Acta **13** (1974), 944–948.
[22] A. V. Ramamurthy, *Wall slip in viscous fluids and influence of materials of construction*, J. Rheol. **30** (1986), no. 2, 337–357.
[23] I. J. Rao, *Flow of a Johnson-Segalman fluid between rotating co-axial cylinders with and without suction*, Internat. J. Non-Linear Mech. **34** (1999), 63–70.
[24] I. J. Rao and K. R. Rajagopal, *Some simple flows of a Johnson-Segalman fluid*, Acta Mech. **132** (1999), no. 1-4, 209–219.
[25] A. H. Shapiro, M. Y. Jaffrin, and S. L. Weinberg, *Peristaltic pumping with long wavelengths at low Reynolds number*, J. Fluid Mech. **37** (1969), no. 4, 799–825.
[26] A. M. Siddiqui, A. Provost, and W. H. Schwarz, *Peristaltic pumping of a second order fluid in a planar channel*, Rheol. Acta **30** (1991), 249–262.
[27] A. M. Siddiqui and W. H. Schwarz, *Peristaltic pumping of a third order fluid in a planar channel*, Rheol. Acta **32** (1993), 47–56.
[28] ———, *Peristaltic flow of a second-order fluid in tubes*, J. non-Newtonian Fluid Mech. **53** (1994), 257–284.

[29] L. M. Srivastava and V. P. Srivastava, *Peristaltic transport of blood; Casson model-II*, J. Biomech. **17** (1984), 821–829.

[30] S. Takabatake and K. Ayukawa, *Numerical study of two-dimensional peristaltic flows*, J. Fluid Mech. **122** (1982), 439–465.

[31] S. Takabatake, K. Ayukawa, and A. Mori, *Peristaltic pumping in circular cylindrical tubes: a numerical study of fluid transport and its efficiency*, J. Fluid Mech. **193** (1988), 269–283.

T. Hayat: Mathematics Department, Quaid-i-Azam University, Islamabad 45320, Pakistan
E-mail address: t_pensy@hotmail.com

Y. Wang: Fachbereich Mechanik, Technische Universität Darmstadt, Hochschulstraße 1, 64289 Darmstadt, Germany
E-mail address: wang@mechanik.tu-darmstadt.de

A. M. Siddiqui: Department of Mathematics, Pennsylvania State University, York, PA 17403, USA
E-mail address: ams5@psu.edu

K. Hutter: Fachbereich Mechanik, Technische Universität Darmstadt, Hochschulstaße 1, 64289 Darmstadt, Germany
E-mail address: hutter@mechanik.tu-darmstadt.de